JACS
JOURNAL OF THE AMERICAN CHEMICAL SOCIETY

COMMUNICATION

pubs.acs.org/JACS

Bioresponsive Mesoporous Silica Nanoparticles for Triggered Drug Release

Neetu Singh,[†,‡] Amrita Karambelkar,[§] Luo Gu,[⊥] Kevin Lin,[‡,§] Jordan S. Miller,[∥] Christopher S. Chen,[∥] Michael J. Sailor,[⊥] and Sangeeta N. Bhatia*[,†,‡,▽,#]

[†]Harvard−MIT Division of Health Sciences and Technology, [‡]The David H. Koch Institute for Integrative Cancer Research, and [§]Department of Chemical Engineering, Massachusetts Institute Technology, Cambridge, Massachusetts 02139, United States

[⊥]Department of Chemistry and Biochemistry, University of California, San Diego, La Jolla, California 92093, United States

[∥]Department of Bioengineering, University of Pennsylvania, Philadelphia, Pennsylvania 19104, United States

[▽]Electrical Engineering and Computer Science, Massachusetts Institute Technology, Cambridge, Massachusetts 02139, United States, and Division of Medicine, Brigham and Women's Hospital, Boston, Massachusetts 02115, United States

[#]Howard Hughes Medical Institute, Cambridge, Massachusetts 02139, United States

Supporting Information

ABSTRACT: Mesoporous silica nanoparticles (MSNPs) have garnered a great deal of attention as potential carriers for therapeutic payloads. However, achieving triggered drug release from MSNPs *in vivo* has been challenging. Here, we describe the synthesis of stimulus-responsive polymer-coated MSNPs and the loading of therapeutics into both the core and shell domains. We characterize MSNP drug-eluting properties *in vitro* and demonstrate that the polymer-coated MSNPs release doxorubicin in response to proteases present at a tumor site *in vivo*, resulting in cellular apoptosis. These results demonstrate the utility of polymer-coated nanoparticles in specifically delivering an antitumor payload.

Nanotechnology has the potential to impact many long-standing challenges in medicine, such as selective drug delivery and sensitive detection of disease.[1−4] In recent years, mesoporous silica nanoparticles (MSNPs) have attracted attention as a promising component of multimodal nanoparticle systems.[5−9] MSNPs are excellent candidates for many biomedical applications owing to their straightforward synthesis, tunable pore morphologies, facile functionalization chemistries, low-toxicity degradation pathways in the biological milieu, and capacity to carry disparate payloads (molecular drugs, proteins, other nanoparticles) within the porous core.[5−8,10−12]

Despite their promise, however, recent reports highlight the potential toxicity of unmodified MSNPs due to interactions of surface silanols with cellular membranes.[13−16] This toxicity can be reduced by coating the nanoparticle with a polymer shell.[5,17−21] Polymer shells also provide colloidal stability, handles for chemoligation (targeting moieties) and improved blood circulation lifetimes, which are crucial for efficient *in vivo* drug delivery. Unfortunately, the polymer shell also limits both drug loading and release from MSNPs.

In order to address the drawbacks of coating, we developed an MSNP polymer that degrades in response to external stimuli. We explored both physical triggers, such as temperature, and biochemical triggers, such as proteases found in the tumor microenvironment. Loading and responsive drug release were explored using payloads incorporated into the MSNP core as well as the polymer shell.

In our attempt to coat MSNPs with polymers, we considered previously reported approaches, such as noncovalent assembly or surface-initiated polymerizations techniques.[18,22−26] These methods, however, have limitations. Noncovalent strategies are prone to colloidal and biological instability, whereas covalent surface-initiated polymerization approaches typically result in larger particles and expose the MSNP to harsh reaction conditions. Furthermore, the existing methods do not provide the flexibility to allow drug loading in distinct compartments. We therefore developed a new strategy (Figure 1a) based on a core−shell architecture and an aqueous free radical polymerization technique. We first electrostatically adsorb an acrylamide to the MSNP surface and then utilize the acryl groups to synthesize a covalently cross-linked poly(ethylene glycol) (PEG)-based polymer shell. The covalent cross-linking can provide addition stability to the polymer shell.[27−29] This synthetic strategy provides a covalent polymer shell without the use of catalysts and surfactants and requires mild conditions compatible with a variety of potential biomolecular payloads.

MSNPs were synthesized via co-condensation of silicates, similar to previous reports.[10,30] To coat the anionic surface of the MSNPs, we used bifunctional *N*-(3-aminopropyl) methacrylamide hydrochloride (APMA). The amino group was electrostatically bound to the nanoparticle surface, while the acrylamide group was available for radical polymerization. Subsequently, a covalently cross-linked polymer shell was synthesized at room temperature by radical polymerization of monomers, including *N*-isopropylacrylamide (NIPAm) or poly(ethylene glycol) diacrylate (PEGDA). The monomer concentrations during synthesis were kept low and in order to produce a dense polymer shell, it was necessary to perform a second polymerization step to yield a "double-coated" nanoparticle.

Transmission electron microscopy (TEM) images (Figure 1b and Figure S1c, Supporting Information) indicated that the synthesis yielded individually encapsulated MSNPs displaying a

Received: August 1, 2011
Published: October 07, 2011

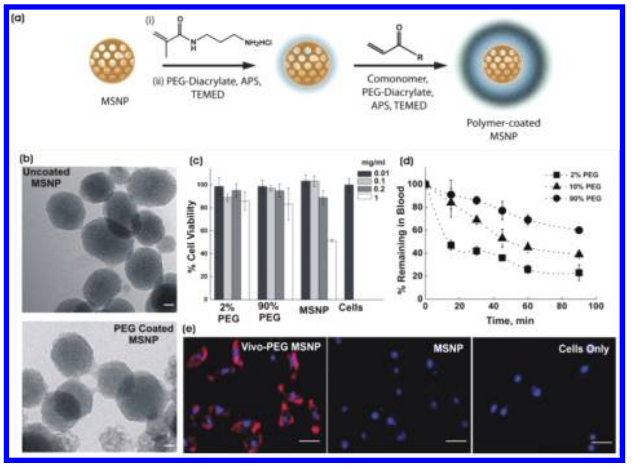

Figure 1. Polymer-coated MSNPs: (a) Synthetic scheme for the polymer coating of MSNPs. (b) TEM micrographs of uncoated and PEG-coated MSNPs. Scale bar is 20 nm. (c) *In vitro* viability of HeLa cells in the presence of uncoated MSNPs and polymer-coated MSNPs ($n = 3$). (d) *In vivo* circulation lifetime of polymer-coated MSNPs after tail vein injections in Swiss Webster mice ($n = 3$). (e) Cellular uptake of PEG−MSNPs by HeLa cells. Red, Vivo Tag 680 conjugated to the polymer shell; Blue, DAPI. Scale bar is 10 μm.

thin polymeric shell, which is absent on uncoated nanoparticles. TEM measurements indicated that the diameters of the uncoated and polymer-coated MSNPs were 70 ± 8 and 94 ± 12 nm, respectively. Dynamic light scattering measurements showed that the hydrodynamic diameter of the MSNPs increased upon addition of single or double pNIPAm-*co*-PEG (9:1 molar ratio) shells by ∼20−40% (Figure S1, Supporting Information). The DLS and TEM data indicate that this polymer coating procedure avoids agglomeration of the nanoparticles into the larger (micrometer-scale) aggregates that have been previously observed with other coating techniques.[22]

We next investigated the drug-loading capacity of the polymer-coated MSNPs by comparing the total amount of drug loaded before and after polymer coating. We chose doxorubicin (Dox) as a model payload due to its well-characterized spectral characteristics, its use in chemotherapy, and its affinity for the negatively charged surface of the silica nanoparticles, which enhances loading into the MSNP pores.[31] The loading of Dox in polymer-coated MSNPs was only slightly lower (∼50% of total Dox added) compared with the uncoated MSNPs (∼60% of total Dox added) (Figure S3a, Supporting Information). This suggests that the polymer shell does not reduce the drug loading capacity of MSNPs as drastically as other reported polymer shell−MSNP systems, which is an additional advantage of our technique over previously reported coating methods.[17,32] We also observed that the polymer shell provided colloidal stability at low pH and prevented aggregation of the MSNPs, which are prone to interparticle hydrogen bonding (Figure S4a, Supporting Information). The synthesis allows facile incorporation of comonomers that can add additional functionality to the shell (Figure S4b, Supporting Information).

To assess the *in vitro* safety and biocompatibility of the polymer-coated MSNPs, we analyzed mitochondrial activity of HeLa cells following incubation with differing concentrations of polymer-coated MSNPs. No significant *in vitro* cytotoxicity was observed for nanoparticle concentrations of 0.01−1 mg/mL and with a range of PEG content in the polymer shell (Figure 1c). By contrast, the uncoated MSNPs exhibited signs of cytotoxicity at concentrations of 1 mg/mL.[13,33]

To study the biological trafficking of the polymer-coated MSNPs, the outer polymer shell was tagged following polymerization with the near-infrared (near-IR) dye Vivo Tag 680. For this formulation, the inner shell consisted of PEGDA and the outer shell was a copolymer of 10 mol % APMA with PEGDA. The dye was conjugated to the free amine side chains on the APMA comonomer. Labeled MSNPs were used to study blood circulation properties *in vivo* and cellular uptake of the nanoparticles *in vitro*. Compared with uncoated MSNPs, PEGylated MSNPs have been shown to possess a longer blood-circulation lifetime and lower excretion of degradation products in the urine.[14] In the present work, increasing the mole percent of PEG from 2 to 90 in the polymer shell increased the circulation lifetime of MSNPs, measured by quantifying Vivo Tag 680 fluorescence in capillary blood draws (Figure 1d). Cellular uptake studies (Figure 1e) confirmed that the 90 mol % PEG-coated MSNP formulation (PEG−MSNPs) was internalized by HeLa cells after 4 h of incubation.

In addition to providing colloidal stability, functional groups for chemical ligation, and improved biocompatibility and blood circulation lifetimes, the polymer shell can be used to impart stimuli responsive characteristics to MSNPs. Stimulus-responsive nanoparticles have been shown to be extremely useful for controlled drug release.[17,34,35] These systems overcome several current delivery challenges in therapy because they can be utilized for sustained drug delivery and co-delivery of multiple drugs with distinct release profiles. In this work, we engineered these long-circulating, biocompatible polymer-coated MSNPs to respond to temperature and the biological microenvironment (protease) for controlled drug delivery.

The thermally responsive system was synthesized from NIPAm−PEG (9:1)-coated MSNPs, and doxorubicin was used as the test drug. It has been shown that pNIPAm, which possesses a lower critical solution temperature (LCST) of ∼31 °C, can provide temperature-triggered release of drugs from various nanoparticles.[35] Consistent with these prior results, at temperatures greater than the LCST (37 °C), about 50% more Dox was released within the first 2 h of incubation, compared with the same formulation maintained at room temperature (Figure 2a). By comparison, uncoated MSNPs released the same quantity of Dox at either temperature.

We further investigated the influence of the polymer shell on the drug release profiles from MSNPs in which the drug was loaded in either the inorganic core or the polymer shell of the nanoparticle. To compare these two loading strategies, we measured the drug loading efficiencies and characterized the drug release profiles in core-loaded and shell-loaded PEG−MSNPs. For the core-loaded PEG−MSNPs, doxorubicin was loaded in the MSNPs with a single PEGDA shell and a second covalent polymer shell (PEG-*co*-APMA) was synthesized after drug loading to provide a diffusion barrier. For the shell-loaded PEG−MSNPs, Dox was loaded after the synthesis of the second PEG-*co*-APMA shell. Excess unloaded Dox was removed by centrifugation of the loaded nanoparticles. Compared with uncoated MSNPs, the loading efficiency of the polymer-coated MSNPs was reduced somewhat but was not dramatically different ($p = 0.043$ by ANOVA tukey analysis, Figure S3b, Supporting Information). Interestingly, the polymer-coated MSNPs held comparable amounts of Dox in either core- or shell-loaded formulations (Figure S3b, Supporting Information). Core-loaded PEG−MSNPs displayed the slowest rate of Dox release; only ∼20% of the

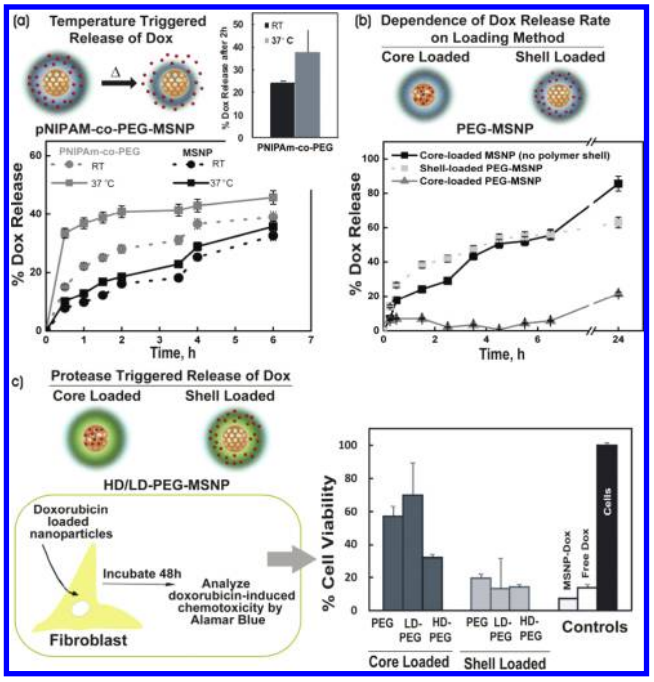

Figure 2. Controlling drug release from polymer-coated MSNPs: (a) Temperature-triggered release of doxorubicin from pNIPAM-co-PEG coated MSNPs. Inset shows release after 2 h. (b) Doxorubicin release profile in PBS at 37 °C for uncoated MSNPs and core-loaded and shell-loaded PEG−MSNPs. (c) Dox-induced chemotoxicity on J2-3T3 fibroblasts from MMP-degradable PEG−MSNPs (HD, highly degradable; LD, low degradability), PEG−MSNPs, and Dox-loaded MSNPs (MSNP-Dox) (n = 3).

drug was released after 24 h (Figure 2b). The shell-loaded PEG−MSNPs released ∼40% of the drug in the first 2 h and ∼60% after 24 h. Initially, the uncoated MSNPs released Dox at a slightly slower rate compared with the shell-loaded PEG−MSNPs but a larger total quantity of drug was released after 24 h (∼85% vs 63% of the loaded drug, respectively). The initial rapid rate of drug release from the shell-loaded PEG−MSNPs compared with the uncoated MSNPs suggested that Dox was loaded both in the core and the polymer shell in this PEG−MSNP formulation. The initial relatively rapid rate of release observed is attributed to diffusion of Dox loaded in the PEG shell. The release of Dox from a formulation in which the drug was loaded exclusively in the MSNP core and then coated with a polymer shell (core-loaded PEG−MSNPs) was much slower. Thus, the polymer shell provides a facile means to tune the drug release profile. The core-loaded PEG−MSNPs display a very slow drug release profile with no premature ("burst") release, both desirable attributes for a "triggered" formulation designed to respond to specific tumoral extracellular signatures, such as proteases. For instance, it is known that matrix metalloproteinases (MMPs), which have the ability to degrade the extracellular matrix, are up-regulated in tumor environments because of secretion by rapidly dividing cancer cells and stromal cells.[34]

We therefore investigated whether MMP proteases could trigger drug release from the polymer-coated MSNPs. For the protease-sensitive polymer shell, we used PEGDA−peptide macromer possessing MMP substrate polypeptides with a highly degradable (HD-MMP) and a low-degradability (LD-MMP) sequence.[36] We investigated protease-triggered drug release from core-loaded or shell-loaded PEG−peptide (HD-MMP and LD-MMP)-coated MSNPs by analyzing the chemotoxicity of Dox released during 48 h of incubation with 3T3-J2 fibroblasts.

In a typical experiment, 3T3-J2 fibroblasts were incubated with nanoparticles and assayed for cell viability using alamarBlue 48 h later. We observed high levels of Dox-induced chemotoxicity (∼15−20% cell viability) in all shell-loaded nanoparticles, regardless of their polymeric shell (PEGDA, LD-MMP, or HD-MMP; Figure 2c). This level of chemotoxicity was comparable to Dox-loaded uncoated MSNPs and free drug (for the same quantity of Dox administered) and is in accordance with the fast drug release profile of shell-loaded and uncoated MSNPs. In contrast, the Dox-induced chemotoxicity of core-loaded PEG−MSNPs was dependent on polymer shell composition. Low level of chemotoxicity (∼60−70% cell viability) was observed for core-loaded PEG−MSNP and LD-PEG−MSNPs, suggesting that in 48 h, the quantity of drug released from low- and nondegradable PEG nanoparticles was limited. Residual levels of drug release from LD-PEG−MSNPs is attributed to leaching of the drug and not cleavage of the PEG−peptide shell. In contrast, the chemotoxicity of core-loaded HD-PEG−MSNPs was high (30% cell viability), signifying that rapid Dox release resulted from cleavage of the PEG−peptide shell by endogenous MMPs in the cellular medium. Indeed, blocking the endogenous MMPs secreted by the fibroblasts with the inhibitor batimastat lowered the chemotoxicity of the HD-MMP−MSNPs (Figure S5b, Supporting Information). These results demonstrate that protease-triggered release can be achieved with polymer-coated MSNPs. The various polymer coatings on MSNPs thus allowed both spatial control over loading and temporal control over release of Dox *in vitro*.

Finally, we conducted *in vivo* studies in subcutaneous xenograft mouse models to test the protease-triggered release of Dox from the polymer-coated MSNPs. We injected a human sarcoma cell line (HT-1080), known to have elevated levels of MMPs,[37] subcutaneously in flanks of immune-compromised mice (Figure 3a). Two weeks later, core-loaded HD-PEG−MSNPs, core-loaded PEG−MSNPs, uncoated MSNPs and Dox-loaded uncoated MSNPs were normalized to a drug concentration of 2 mg/kg and injected into well-defined tumors. The tumors were removed after 60 h and analyzed for Dox-induced apoptosis by measurement of TUNEL staining and caspase levels (Figure 3b,c). Tumor cell lysates were analyzed for apoptosis markers procaspase-9 and cleaved caspase-9 by immunoblotting (Figure 3b). While the GAPDH levels were similar for each sample, exposure to the core-loaded HD-PEG−MSNP formulation and Dox-loaded uncoated MSNPs generated higher levels of the caspases. In contrast, the core-loaded PEG−MSNPs showed lower caspase levels, similar to those of saline-treated samples. Interestingly, core-loaded PEG−MSNPs generated lower levels of caspases compared with unloaded uncoated MSNPs. This finding is in accordance with *in vitro* studies suggesting that the polymer shell reduces inherent nanoparticle toxicity. TUNEL staining of the tumor sections (Figure 3c) indicated that the core-loaded HD-PEG−MSNPs mediated significantly higher Dox-induced cell death compared with PEG−MSNPs. Taken together, these results show that the core-loaded MSNPs with an MMP-sensitive PEG shell exhibit higher Dox-induced chemotoxicity than those with a non-MMP-sensitive PEG shell. We conclude that this higher chemotoxicity is due to efficient release of Dox triggered by the MMPs *in vivo*. This system takes advantage of the ability of the PEG polymer shell to reduce the inherent toxicity of MSNPs, and incorporation of a protease-cleavable moiety achieves triggered delivery that accelerates tumor-localized drug release.

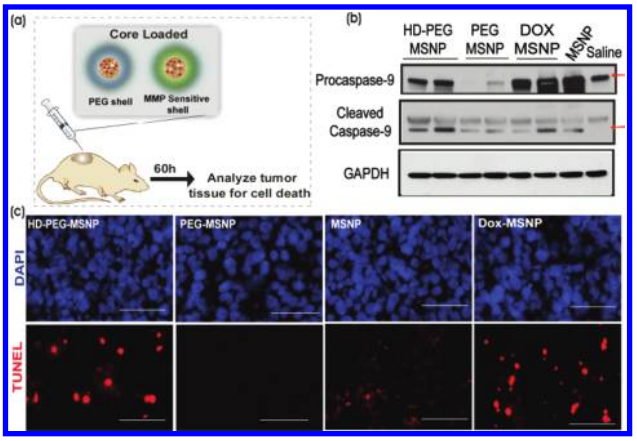

Figure 3. Protease-triggered release of Dox *in vivo*: (a) Schematic for evaluating protease-triggered release from core-loaded MSNPs. (b) Immunoblots for protein levels of caspases (apoptotic markers) and GAPDH from tumor lysates of animals 60 h after treatment. (c) TUNEL staining for apoptotic cells in tumor sections. Red, TUNEL; blue, DAPI. Scale is 50 μm.

In conclusion, we reported a facile and versatile method for coating MSNPs with responsive, biocompatible polymers. The polymer shell not only enables functionalization of the MSNPs with various ligands but also provides colloidal stability, temperature sensitivity, imaging capability, longer blood circulation, high payload capacity, and the opportunity to tune the loading and release of small molecules. Furthermore, we demonstrated that the polymer shell can be used to achieve predetermined, temporal control over drug release; the appropriately modified polymer can be responsive to endogenous proteases allowing triggered, localized drug release *in vitro* and *in vivo*. The polymer coatings also allow spatial control of payload loading within the nanostructure of the MSNP. This capacity is important for applications requiring multiple payloads with specifically timed release profiles from a single nanoparticle system.

■ ASSOCIATED CONTENT

Supporting Information. Detailed experimental procedures, figures and complete refs 5 and 37. This material is available free of charge via the Internet at http://pubs.acs.org.

■ AUTHOR INFORMATION

Corresponding Author
sbhatia@mit.edu

■ ACKNOWLEDGMENT

We acknowledge financial support from the NIH through Grants R01-CA124427, U54-CA119349, and U54-CA119335. This material is based upon work supported by the NSF Grant No. DMR-0806859. We thank Swanson Biotechnology Center at the KI-MIT. We thank Justin Lo for discussions about the manuscript and figures. S.N.B. is an HHMI Investigator. A.K. acknowledges support from Amgen-UROP Scholars Program at MIT.

■ REFERENCES

(1) Farokhzad, O. C.; Langer, R. *ACS Nano* **2009**, *3*, 16.
(2) Shi, J.; Votruba, A. R.; Farokhzad, O. C.; Langer, R. *Nano Lett.* **2010**, *10*, 3223.
(3) Xia, Y. *Nat. Mater.* **2008**, *7*, 758.
(4) Byrne, J. D.; Betancourt, T.; Brannon-Peppas, L. *Adv. Drug Delivery Rev.* **2008**, *60*, 1615.
(5) Ashley, C. E.; et al. *Nat. Mater.* **2011**, *10*, 389.
(6) Slowing, I. I.; Trewyn, B. G.; Giri, S.; Lin, V. S. Y. *Adv. Funct. Mater.* **2007**, *17*, 1225.
(7) Slowing, I. I.; Vivero-Escoto, J. L.; Trewyn, B. G.; Lin, V. S. Y. *J. Mater. Chem.* **2010**, *20*, 7924.
(8) Wu, S.-H.; Lin, Y.-S.; Hung, Y.; Chou, Y.-H.; Hsu, Y.-H.; Chang, C.; Mou, C.-Y. *ChemBioChem* **2008**, *9*, 53.
(9) Liong, M.; Angelos, S.; Choi, E.; Patel, K.; Stoddart, J. F.; Zink, J. I. *J. Mater. Chem.* **2009**, *19*, 6251.
(10) Trewyn, B. G.; Slowing, I. I.; Giri, S.; Chen, H.-T.; Lin, V. S. Y. *Acc. Chem. Res.* **2007**, *40*, 846.
(11) Vivero-Escoto, J. L.; Slowing, I. I.; Trewyn, B. G.; Lin, V. S. Y. *Small* **2009**, *6*, 1952.
(12) Tasciotti, E.; Liu, X.; Bhavane, R.; Plant, K.; Leonard, A. D.; Price, B. K.; Cheng, M. M.-C.; Decuzzi, P.; Tour, J. M.; Robertson, F.; Ferrari, M. *Nat. Nanotechnol.* **2008**, *3*, 151.
(13) Chang, J.-S.; Chang, K. L. B.; Hwang, D.-F.; Kong, Z.-L. *Environ. Sci. Technol.* **2007**, *41*, 2064.
(14) He, Q.; Zhang, Z.; Gao, F.; Li, Y.; Shi, J. *Small* **2010**, *7*, 271.
(15) He, Q.; Zhang, Z.; Gao, Y.; Shi, J.; Li, Y. *Small* **2009**, *5*, 2722.
(16) Lin, Y.-S.; Haynes, C. L. *J. Am. Chem. Soc.* **2010**, *132*, 4834.
(17) Gao, Q.; Xu, Y.; Wu, D.; Sun, Y.; Li, X. *J. Phys. Chem. C* **2009**, *113*, 12753.
(18) Muhammad, F.; Guo, M.; Qi, W.; Sun, F.; Wang, A.; Guo, Y.; Zhu, G. *J. Am. Chem. Soc.* **2011**, *133*, 8778.
(19) Song, S. W.; Hidajat, K.; Kawi, S. *Chem. Commun.* **2007**, 4396.
(20) Thornton, P. D.; Heise, A. *J. Am. Chem. Soc.* **2010**, *132*, 2024.
(21) Zhao, Y.; Trewyn, B. G.; Slowing, I. I.; Lin, V. S. Y. *J. Am. Chem. Soc.* **2009**, *131*, 8398.
(22) Huang, S.; Fan, Y.; Cheng, Z.; Kong, D.; Yang, P.; Quan, Z.; Zhang, C.; Lin, J. *J. Phys. Chem. C* **2009**, *113*, 1775.
(23) Lu, J.; Liong, M.; Zink, J. I.; Tamanoi, F. *Small* **2007**, *3*, 1341.
(24) Popat, A.; Hartono, S. B.; Stahr, F.; Liu, J.; Qiao, S. Z.; Qing Lu, G. *Nanoscale* 2011, 3, 2801.
(25) Sun, J.-T.; Hong, C.-Y.; Pan, C.-Y. *J. Phys. Chem. C* **2010**, *114*, 12481.
(26) Yang, Y.; Yan, X.; Cui, Y.; He, Q.; Li, D.; Wang, A.; Fei, J.; Li, J. *J. Mater. Chem.* **2008**, *18*, 5731.
(27) Joralemon, M. J.; O'Reilly, R. K.; Hawker, C. J.; Wooley, K. L. *J. Am. Chem. Soc.* **2005**, *127*, 16892.
(28) Choi, W. I.; Yoon, K. C.; Im, S. K.; Kim, Y. H.; Yuk, S. H.; Tae, G. *Acta Biomater.* **2010**, *6*, 2666.
(29) Wang, Y.; Bansal, V.; Zelikin, A. N.; Caruso, F. *Nano Lett.* **2008**, *8*, 1741.
(30) Lai, C.-Y.; Trewyn, B. G.; Jeftinija, D. M.; Jeftinija, K.; Xu, S.; Jeftinija, S.; Lin, V. S. Y. *J. Am. Chem. Soc.* **2003**, *125*, 4451.
(31) Prokopowicz, M.; Przyjazny, A. *J. Microencapsulation* **2007**, *24*, 694.
(32) Shi, X.; Wang, Y.; Varshney, R. R.; Ren, L.; Zhang, F.; Wang, D.-A. *Biomaterials* **2009**, *30*, 3996.
(33) He, Q.; Zhang, J.; Shi, J.; Zhu, Z.; Zhang, L.; Bu, W.; Guo, L.; Chen, Y. *Biomaterials* **2010**, *31*, 1085.
(34) Danhier, F.; Feron, O.; Préat, V. *J. Controlled Release* **2010**, *148*, 135.
(35) Yavuz, M. S.; Cheng, Y.; Chen, J.; Cobley, C. M.; Zhang, Q.; Rycenga, M.; Xie, J.; Kim, C.; Song, K. H.; Schwartz, A. G.; Wang, L. V.; Xia, Y. *Nat. Mater.* **2009**, *8*, 935.
(36) Miller, J. S.; Shen, C. J.; Legant, W. R.; Baranski, J. D.; Blakely, B. L.; Chen, C. S. *Biomaterials* **2010**, *31*, 3736.
(37) Albright, C. F.; et al. *Mol. Cancer Ther.* **2005**, *4*, 751.

Bioresponsive Mesoporous Silica Nanoparticles for Triggered Drug Release

Neetu Singh,[1,2] Amrita Karambelkar,[3] Luo Gu,[4] Kevin Lin,[2,3] Jordan S. Miller,[5] Christopher S. Chen, [5] Michael J. Sailor,[4] Sangeeta N. Bhatia[1,2,6, 7*]

[1]Harvard- MIT Division of Health Sciences and Technology, [2]The David H. Koch Institute for Integrative Cancer Research, [3]Department of Chemical Engineering, Massachusetts Institute Technology, Cambridge, MA, 02139, [4] Department of Chemistry and Biochemistry, University of California, San Diego, La Jolla, CA, 92093, [5] Department of Bioengineering, University of Pennsylvania, Philadelphia, PA, 19104, [6] Electrical Engineering and Computer Science, MIT, Cambridge, MA, 02139, Division of Medicine, Brigham and Women's Hospital, Boston, MA, 02115, [7] Howard Hughes Medical Institute Cambridge, MA, 02139

Materials. All materials were obtained from Sigma Aldrich unless otherwise specified and were used as received. HeLa-GFP and HT-1080 cells were cultured in Dulbecco's modification of Eagl'es medium (DMEM, purchased from Invitrogen) with 10% bovine serum (Invitrogen), 5 I.U. penicillin, and 5 µg/mL streptomycin. 3T3-J2 Fibroblast cells were cultured in Dulbecco's modification of Eagl'es medium (DMEM, purchased from Invitrogen) with 10% bovine serum (Invitrogen), 5 I.U. penicillin, and 5 µg/mL streptomycin. All animal work was performed in accordance with the institutional animal protocol guidelines in place at the Massachusetts Institute of Technology, and it was reviewed and approved by the Institute's Animal Research Committee.

Synthesis of mesoporous silica nanoparticles: To a 1g CTAB in NaOH (14 mM) at 80 °C, was added 5 mL TEOS and 5 µL APTES. The solution was stirred at 80 °C for 2 h to produce the white MSNPs suspension. The product was washed with methanol and water several times and then refluxed for 6 h in HCl/methanol to extract the CTAB. The Final MSNPs were then again washed several times with methanol and water and dried in air.

Synthesis of on-surface polymer-coated silica nanoparticles: For synthesizing single coated MSNPs, a 2 mg/mL solution of MSNPs was prepared in distilled water (DI) and sonicated to disperse the particles until a uniform colloidal solution was observed. To this solution 1 M of N-(3-Aminopropyl)methacrylamide hydrochloride, or APMA (Polysciences, Inc.) was added and left on the shaker table overnight. The solution was then centrifuged at 13200 rpm for 10 minutes to remove excess APMA. Next a 6 mM total monomer solution with an appropriate amount of monomers in DI water was added to the reaction vial. . The total monomer concentration used in forming the shell was necessarily kept very low (<8 mM) to avoid encapsulation of multiple MSNPs in the polymer matrix. Monomers that were used included: poly(ethylene glycol)

diacrylate (PEGDA, molecular weight 700), N-Isopropylacrylamide (NIPAM), PEG-MMP-HD, PEG-MMP-LD. Amine functionality was incorporated by copolymerizing APMA, which was 10% by mole of the total monomer concentration. For polymer shell containing Coumarin, a hydrophobic, fluorescent comonomer 7-[4-(Trifluoromethyl) coumarin] methacrylamide dissolved in dimethyl sulfoxide was added to the reaction vial. For NIPAm based polymer shells, a molar composition of 80% monomer (NIPAM), 10% crosslinker (PEG-DA) and 10% comonomer was used. For PEG based polymer shells, 90% PEGDA and 10% of comonomer was used. The total monomer concentration used for all the polymer shell synthesis was 6 mM. After addition of all the monomers, 1.3% by volume of 0.1 M ammonium persulfate (APS) was added. After thorough mixing by vortex, the polymerization reaction was initiated by adding 1% by volume N,N,N′,N′-Tetramethylethylenediamine (TEMED). The reaction solution was stirred overnight. The solution was then centrifuged at 13200 rpm for 10 minutes and resuspended in DI water to remove excess unreacted monomers and initiators. The synthesized polymer coated MSNPs were cleaned by several such cycles of centrifugation/resuspension. The clean single-polymer coated MSNPs can then be used for synthesizing multiple polymer shells using the same procedure. The single-coated polymer-MSNPs can further be used to obtain core-loaded MSNPs, by adding doxorubicin hydrochloride to the cleaned nanoparticles. Doxorubicin was added at a concentration of 60 μg/mg MSNPs. A second polymer shell was then synthesized on the cleaned Dox loaded single-coated MSNPs by following the same procedure outlined above. If a Dox loaded polymer-MSNPs were used, then the second shell polymerization was carried out in a1mg/ml doxorubicin solution in DI water. For synthesizing the second polymer shell on unloaded polymer coated MSNPs, the reaction was carried out in just DI water. For shell-loaded MSNPs, the two polymer coats were synthesized first and the double-coated MSNPs were then

incubated with doxorubicin at a doxorubicin concentration of 60 μg/mg MSNPs. To create Vivotag 680®-tagged MSNPs, after the polymer shell synthesis with APMA as comonomer, 5X molar excess of amine reactive Vivotag 680® NHS were added to the cleaned polymer-MSNP pellet and reacted for at least 4 hours. After every synthesis step and doxorubicin loading steps, the MSNPs were cleaned via several cycles of centrifugation and resuspension to remove unreacted monomers, excess reagents, and soluble reaction byproducts. The particle size of the synthesized polymer-MSNPs was characterized by dynamic light scattering instrument (Zetasizer-Nano, Malvern, Inc.). The data presented is an average of 3 experiments with at least 50 measurements in each experiment. We found that the nanoparticle size and polymer thickness could be controlled by the monomer concentration used for polymerization (Figure S1a,b), thus providing synthetic flexibility.

Synthesis of MMP-sensitive acrylate–PEG–(peptide–PEG)m–acrylate Macromers: The bis-cysteine peptide sequences CGPQGIWGQGCR (highly degradable, HD, 1261.42 g/mol), CGPQGIAGQGCR (native collagen, NC, 1146.28 g/mol), and CGPQGPAGQGCR (least degradable, LD, 1130.23 g/mol) were custom synthesized by Aapptec (Louisville, KY). In a typical reaction, 183.8 mmol biscysteine peptide (HD, 231.6 mg) was reacted with a 1.6 molar excess of PEGDA (3400 Da, 1 g, 294.1 mmol) by dissolution in 10 mL 100 mM sodium phosphate, pH 8.0 (94.7 mM Na2HPO4, 5.3 mM NaH2PO4). The reaction was sterile filtered through a 0.22 mm PVDF membrane (Millipore, Billerica, MA), protected from light and proceeded on a circular shaker for 85 h at room temperature to yield acrylate–PEG–(peptide–PEG)m–acrylate macromers. The reaction mixture was dialyzed against DI water (Millipore) with regenerated cellulose dialysis tubing (MWCO 3500, Pierce, Rockford, IL) for 24 h with

water changes every 4 h. The dialyzed PEG–peptide conjugates were frozen overnight (-20 °C), lyophilized, and stored at -80 °C until use. The degradability of HD-MMP and LD-MMP in solution relative to native collagen was 800% and 0.5% respectively.

Transmission Electron Microscopy: The synthesized nanoparticles were imaged on a JEOL 200CX (200 kV) transmission electron microscope (TEM). All TEM samples were prepared by casting a drop of the nanoparticle solution (diluted 10 times) on a Formvar-coated Cu TEM grid (Ted Pella) placed on a Kimwipe. The grid was then dried overnight at ambient temperature.

UV-Vis and Fluorescence Spectroscopy: All absorption and fluorescence spectra were obtained in 96Well Clear Flat Bottom UV-Transparent and black 384 well microplates respectively using a Molecular Devices microplate Spectrophotometers.

Drug loading and release: Nanoparticles were incubated with doxorubicin hydrochloride while shaking overnight at a concentration of 60 µg/mg MSNPs. Following incubation, the nanoparticles were centrifuged at 13200 rpm for 10 minutes. The amount of doxorubicin loaded was calculated by obtaining the absorbance of the supernatant and the pellet at 490 nm. For release studies, the doxorubicin-loaded nanoparticle pellet was resuspended in the same volume of distilled water and incubated at room temperature or 37 ºC (for temperature triggered release). After 2 hours the solution was centrifuged at 13200 rpm for 10 minutes and the supernatant absorbance at 490 nm was measured to calculate the percentage of drug released. Release kinetics of the loaded doxorubicin from core loaded and shell loaded polymer-MSNPs (2 mg/mL) in PBS at 37^{o}C was measured by using the Slide-A-Lyzer MINI Dialysis Device (Invitrogen). The dialysis devices were kept in a stirring water bath. At each time point the Dox loaded MSNPs solution were removed and the Dox left in the MSNPs solution was monitored by

measuring the absorbance at 490 nm and the fluorescence at 590 nm (λex = 480 nm). For release of doxorubicin in the presence of collagenase, the nanoparticles were incubated with 0.2 mg/mL collagenase in PBS buffer (pH 7) solution at 37 ºC for specified time. The samples were removed and centrifuged at 13200 rpm for 10 minutes and the absorbance at 490 nm for the supernatant and the pellet were measured to calculate the percentage of drug released.

Cellular uptake study of Vivotag PEG-MSNPs: HeLa cells were cultured on cover slips in a 12-well plate to ~70-80% confluence. To the HeLa cell cultures, 100 µL of Vivotag PEG-MSNPs and bare MSNPs (2mg/ml) were added to each well and incubated for 4 h at 37 °C, after which the nanoparticles were removed and the cells were then rinsed three times with cell medium, fixed with 4% paraformaldehyde for 20 min. The cellular nuclei were stained with DAPI. The fixed and stained cells were then observed under the fluorescence microscope with UV filter cubes and Cy 5 filter cube was used.

Cytotoxicity of nanoparticle formulations: Cytotoxicity assessments were conducted on HeLa cells in 96-well plates grown to ~70-80% confluency. Cells were incubated in triplicate with specified concentrations of the nanoparticles in 10% FBS DMEM medium for 24 h. Cells were then washed three times with cell medium and assessed for viability using the Calcein assay (Invitrogen) and MTT assay according to manufacturer's instructions. Cell viability was expressed as the percentage of viable cells compared with controls (cells without nanoparticles).

In vivo circulation of nanoparticles: Vivo-Tag labeled polymer-MSNPs were injected in Swiss Webster mice through tail-vein injections. Blood (about 100 µl) was periodically drawn retro orbitally and the near-infrared fluorescence from the circulating nanoparticles was measured using the Odyssey imaging system (Li-COR Biosciences). While the PEG-coated MSNPs with 2

mol % PEG and 10 mol % PEG had a blood circulation half-lives of 15 and 45 min, respectively, >60% of the nanoparticles coated with 90% PEG were still in circulation 90 min post-injection.

Cellular cytotoxicity due to Doxorubicin release from MMP responsive MSNPs: 3T3-J2 fibroblast cells were cultured on a 96 well plate at a density of 5000 cells/well. After 36 hours, the MSNPs were added such that the doxorubicin concentration in each well was 8μg/mL. The cells were incubated with nanoparticles for 24h and 48h followed by washing of the cells with cellular medium three times. The cytotoxicity was measured by Alamar blue (invitrogen) assay according to the manufacturer's protocol. Cell viability was expressed as the percentage of viable cells compared with controls (cells without nanoparticles).

In vivo treatment of mouse tumors: All xenograft animal studies were conducted in accordance with guidelines from the MIT Committee on Animal Care with approved protocols. A human sarcoma cell line (HT-1080) were injected subcutaneously in flanks of 4- to 6-week-old NCr/nude mice (Charles River Laboratories) at 5 x 10^6 cells per mouse per tumor. Two weeks after injection, tumor establishment was confirmed by a well established tumor mass. The animals were randomly divided into five cohorts of at least three animals each. The nanoparticles were intratumorally injected at a dose of 2 mg DOX/kg body mass (200 μL in PBS solution). Animals were euthanized 60h after the injection, and tumors were harvested for immunoblotting and histological analyses.

Immunoblotting: Frozen tumor tissues were homogenized in a lysate buffer containing protease inhibitor cocktail (Roche) on ice. The tissue lysates were centrifuged at 12,000 rpm for 20 minutes at 4° C. The supernatants were collected, and their protein concentrations measured with BCA reagents (Pierce, Rockford, Illinois). The proteins in the lyasate were separated by

electrophoresis on a 4-20% acrylamide gel (Bio-Rad) and transferred to a poly(vinylidene diluoride) membrane, which were then blocked with 5% nonfat milk in 0.1% Tween 20-TBS for 2 h at room temperature. The membranes were immunoblotted with one of the primary antibodies for caspase-9 (cell signaling) and GAPDH (cell signaling). After further washing, the blots were incubated with the appropriate horseradish peroxidase–conjugated secondary antibody. Antibody binding was detected with the Western Blotting Reagent (Pierce).

Histological (TUNEL) analysis. For histological analysis, frozen sections of tumours were prepared. The sections were first fixed 4% paraformaldehyde and stained with TMR red *in-situ* cell death detection kit (Roche) according to the protocol provided by the manufactures. The slides were counterstained with DAPI and mounted on glass slides for microscopic analysis. At least three images from representative microscopic fields were analyzed for each tumour sample using the ImageJ software.

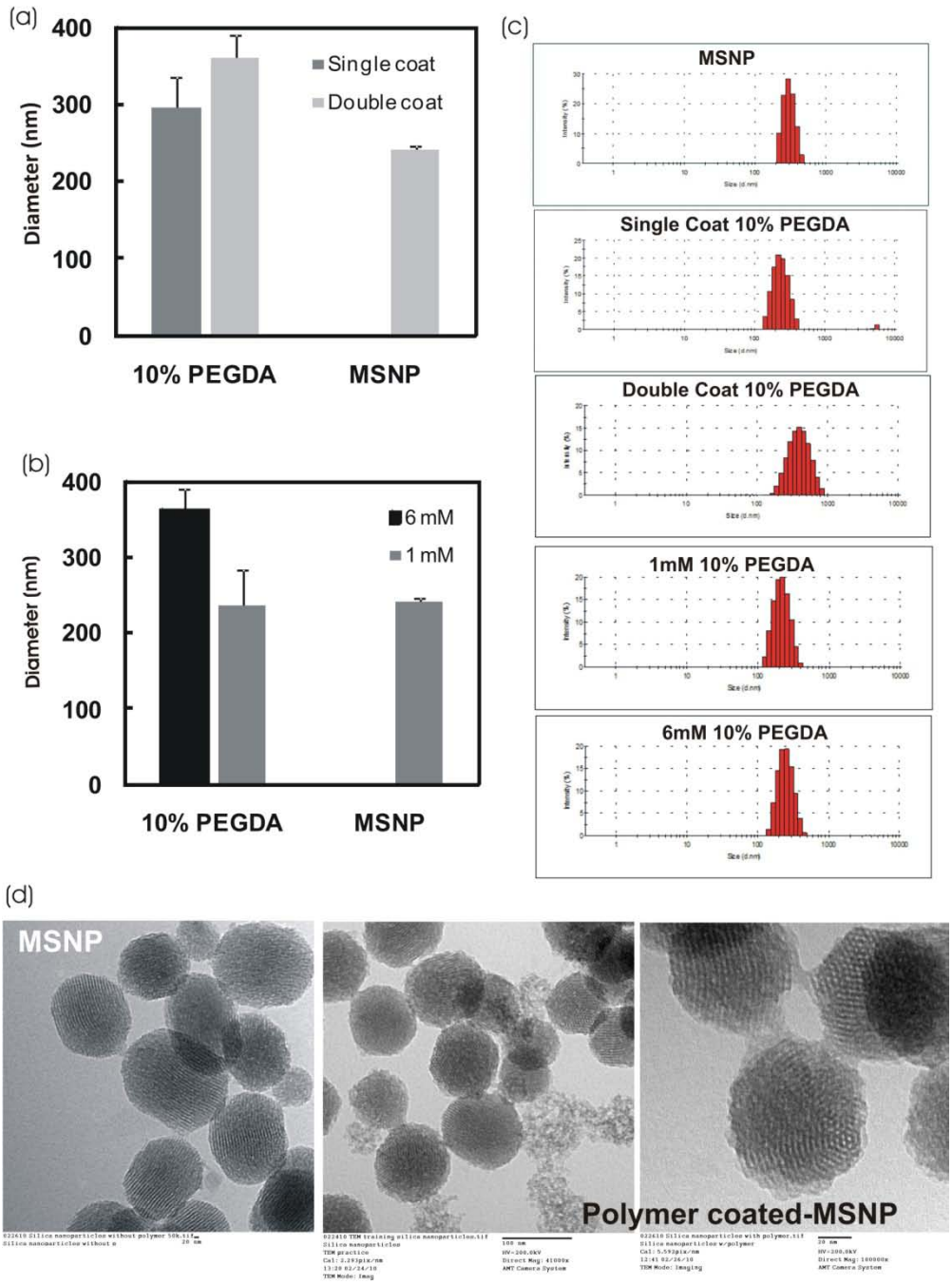

Fig S1: (a) Size of the MSNPs before and after single and double polymer shell as measured by DLS (b) Size of double shell MSNPs with varying polymer concentration. (c) Size histograms of the MSNPs before and after single and double polymer shell as measured by DLS (d) TEM images of polymer-coated MSNPs.

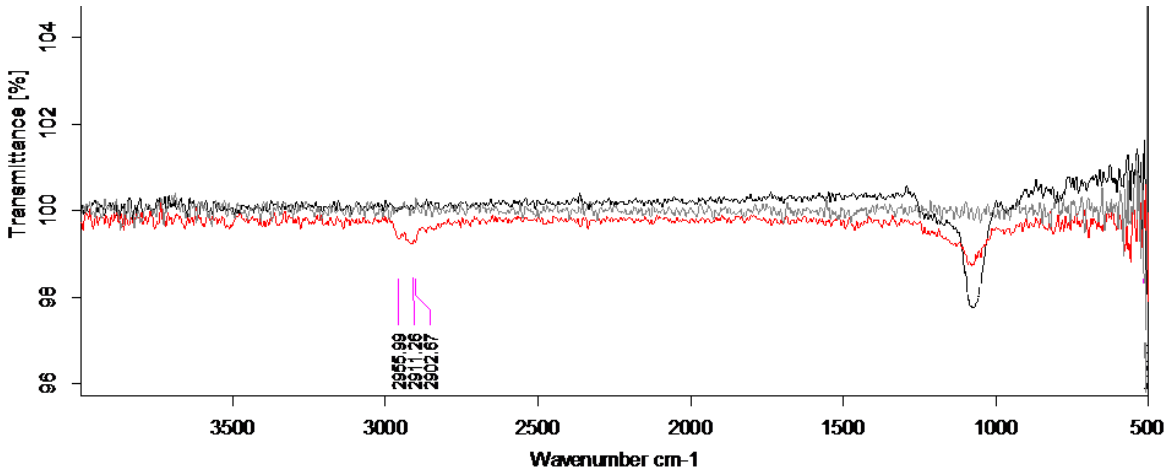

Fig S2: FT-IR spectra of MSNPs before (black) and after polymer shell coating (red).

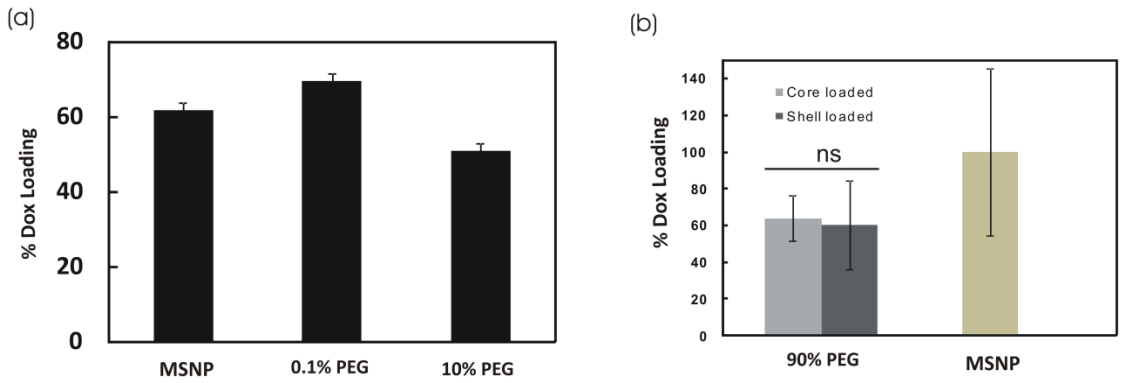

Fig S3: (a) Doxorubicin loading in (a) uncoated, 0.1% and 10% PEG coated MSNPs. (b) Relative Dox loading compared to bare MSNPs in PEG-MSNPs by core loading strategy (second shell synthesis after drug loading) and shell loading strategy (drug loading after both shell syntheses). The difference in % Dox loading was not significant (ns) compared to uncoated MSNP (p = 0.043, ANOVA; Tukey's test at 0.05 significance level)

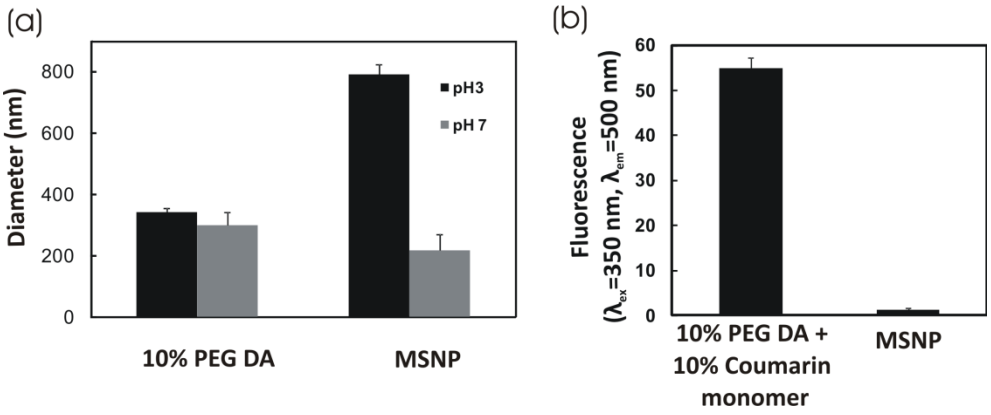

Fig S4: (a) Changes in the size of MSNPs at pH 3 and pH 7 before and after polymer coating. At pH 3 silanols (pKa 126 ≈ 3.5) on the surface of uncoated MSNPs become protonated and the negative repulsive interactions between the particles decrease significantly, resulting in aggregation. In contrast, the MSNPs coated with 10 mol % PEGDA display no significant increase in size at pH 3 compared with pH 7. (b) Fluorescence from coumarin–PEG coated MSNPs. The synthesis allows facile incorporation of comonomers that can add additional functionality to the shell. For example, a hydrophobic fluorescentmonomer (7-[4-(trifluoromethyl) coumarin] methacrylamide) was incorporated along with NIPAm and PEGDA onto the MSNPs

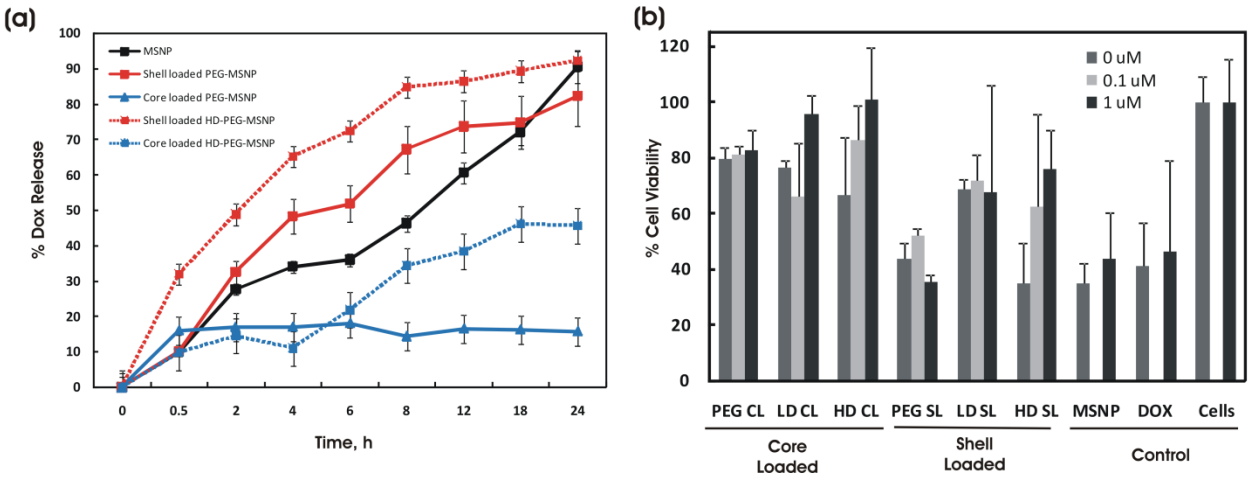

Fig S5: (a) Doxorubicin release profile in PBS at 37 °C for uncoated MSNPs, core-loaded and shell-loaded PEG-MSNPs, core-loaded and shell-loaded HD-PEG-MSNPs in presence of collagenases. (b) Cytotoxicity on J2-3T3 fibroblasts due to released doxorubicin from MMP-degradable PEG-MSNPs (HD: highly degradable; LD: low degradable; CL: core loaded; SL: shell loaded), PEG-MSNPs and uncoated doxorubicin loaded MSNPs in the presence of exogenous batimastat (MMP inhibitor).

Complete References:

(5) Ashley, C. E.; Carnes, E. C.; Phillips, G. K.; Padilla, D.; Durfee, P. N.; Brown, P. A.; Hanna, T. N.; Liu, J.; Phillips, B.; Carter, M. B.; Carroll, N. J.; Jiang, X.; Dunphy, D. R.; Willman, C. L.; Petsev, D.

N.; Evans, D. G.; Parikh, A. N.; Chackerian, B.; Wharton, W.; Peabody, D. S.; Brinker, C. J., Nat Mater 2011, 10, 389.
(37) Albright C. F., Graciani N., Han W., Yue E., Stein R., Lai Z., Diamond M., Dowling R., Grimminger L., Zhang S. Y., Behrens D., Musselman A., Bruckner R., Zhang M., Jiang X., Hu D., Higley A., DiMeo S., Rafalski M., Mandlekar S., Car B., Yeleswaram S., Stern A., Copeland R. A., Combs A., Seitz S. P., Trainor G. L., Taub R., Huang P. and Oliff A., Mol Cancer Ther 2005, 4, 751.